

Article

A Dynamic Heat Pump Model for Indoor Climate Control of a Broiler House

Dimitrios Tyris ¹, Apostolos Gkoutas ², Panteleimon Bakalis ², Panagiotis Panagakis ¹
and Dimitris Manolakas ^{1,*}

¹ Department of Natural Resources Development and Agricultural Engineering, Agricultural University of Athens, 75 Iera Odos Str., 11855 Athens, Greece

² THERMODRAFT IKE, 6 Vasiladiou & Mikalis Str., 18540 Piraeus, Greece

* Correspondence: dman@aua.gr

Abstract: Environment control systems in broiler houses utilize non-renewable electricity and fuels as energy sources, contributing to the increase in greenhouse gases, while not providing optimal conditions. The heat pump (HP) is an energy-efficient technology that can continuously regulate the indoor temperature and relative humidity by combining different operation modes (heating, cooling, and dehumidifying). The current study presents an analytical numerical model developed in Simulink, capable of simulating the thermal loads of a broiler house and the dynamic operation of three heat pumps to cover its needs. Outdoor climatic conditions and broilers' heat production are used as inputs, while all the heat exchange mechanisms with the external environment are considered. The study investigates the energy use and performance of each HP mode under different environmental conditions. A total of 7 different production periods (PPs) are simulated for a 10,000-broiler house in northern Greece, showing total energy consumption of 18.5 kWh/m², 43.4 kWh/m², and 58.7 kWh/m² for heating, cooling, and dehumidifying, respectively. The seasonal coefficient of performance (SCOP) reaches above 3.1 and 4.8 for heating and dehumidifying, respectively, while the seasonal energy efficiency ratio (SEER) for cooling is above 3.7. Finally, focusing on the two warmer periods, a comparison between cooling with and without evaporative pads was performed, showing similar energy consumption.

Keywords: broiler house modeling; heat pump model; animal house environment control; indoor climate control



Citation: Tyris, D.; Gkoutas, A.; Bakalis, P.; Panagakis, P.; Manolakas, D. A Dynamic Heat Pump Model for Indoor Climate Control of a Broiler House. *Energies* **2023**, *16*, 2770. <https://doi.org/10.3390/en16062770>

Academic Editors: Chi-Ming Lai, Ioan Sarbu and Xi Chen

Received: 21 January 2023

Revised: 2 March 2023

Accepted: 14 March 2023

Published: 16 March 2023



Copyright: © 2023 by the authors. Licensee MDPI, Basel, Switzerland. This article is an open access article distributed under the terms and conditions of the Creative Commons Attribution (CC BY) license (<https://creativecommons.org/licenses/by/4.0/>).

1. Introduction

The European Union (EU) is one of the world's largest poultry meat producers and a net exporter of poultry products. The poultry meat sector is one of the most intensive farming systems in the EU, with an annual production of around 13.2 million tons in 2021 [1]. Intensive broiler farming is characterized by high stocking densities, fast growth rates, very large facilities, and indoor rearing. In intensive production systems, chickens are genetically selected for fast growth to achieve the target live weight of 2.0–2.5 kg within 35 to 45 days. This farming model accounts for around 90% of broiler production in the EU [2].

To achieve the optimal growth rate and maximum performance of broilers, while ensuring health and welfare conditions, an effectively controlled indoor environment is a necessity. Among other factors, efficient space heating and cooling are of great importance.

Broilers are homeothermic animals and attempt to maintain their body temperature at constant levels [3,4]. Too-high and too-low ambient temperatures negatively affect their performance by (i) reducing their body weight gain and, (ii) compromising their health and increasing their mortality [5–8]. Exposure to cold temperatures causes harm to their digestive and immune systems [9], leading to decreased growth rate, as well as to increased disease susceptibility. Similarly, in a high-temperature environment their feed

intake, feed efficiency, and growth rate are reduced [10]. Except for the temperature, broilers' homeothermic regulation is also directly affected by relative humidity levels [11]. Therefore, broilers must be housed under thermoneutral conditions in terms of air temperature and relative humidity.

Indoor environmental control is mostly pursued by utilizing conventional technologies and practices [12,13], such as heaters, fans, and evaporative pads. These technologies may result in increased operational costs, high energy dependence on fossil energy sources [14], and increased greenhouse gas (GHG) emissions. Even though the existing energy use data on livestock systems, and—by extension—in the broiler industry, are fragmented, characterized by multiple methodologies and considerable data gaps [15], the high energy use for environment control in broiler houses in Europe is concluded by several studies conducted during the last decade.

It has been indicated that the energy consumption in poultry houses is expected to vary between 60–80 kWh/m²/year, depending not only on the location of the poultry farm but also on the level of the technology installed [16]. It has also been reported that the total annual thermal energy and electrical energy use in broiler houses range from 86–137 kWh/m² and 7–16 kWh/m², respectively [17]. Constantino et al. [18] simulated an entire production cycle, estimating the thermal energy consumption due to heating and the electrical energy consumption due to ventilation (not including cooling), showing a total of 3184 kWh (an underestimation of about 10% compared with the calculations) for space heating, and 5463 kWh (an overestimation of 7.9%, compared with the recorded) for the electrical energy consumption. Of course, energy use calculations depend strongly on the local climatic data and the building construction materials, as well as the heating/cooling technology, and the automation applied [17]. Studies conducted in the Greek region at four poultry farms located in different altitudes and with different technology adoption levels [19] concluded that the average final energy consumption varies from 46.38 kWh/m² (low land/"new technology") to 89.37 kWh/m² (mountainous/"old technology"). In the above-mentioned study, insulated buildings with high automation-level infrastructure are classified as "new technology".

The most commonly used conventional technologies carry inherent limitations in terms of regulating the indoor environment (i.e., not effective control of temperature and relative humidity), often overlooking the strong interactions between broilers and their environment. Moreover, when combined with low-performance, conventional control strategies may lead to additional economic mislaying due to both higher energy use and lower flock performance. Efforts on climate control systems for broiler and animal houses have been made during the last years to demonstrate the requirement of the development of new control techniques, incorporating modern control theory [20], modern supervisory control for closed broilers' houses [21], predictive control for temperature and humidity in a naturally ventilated buildings [22], and optimal control [23]. Several of these approaches are either theoretically perplexing or challenging to implement in a real poultry house system [24]. Even though heating, ventilation, and air conditioning (HVAC) heat pump (HP) systems have already demonstrated their capacity to precisely control the residential buildings' environment, their integration in animal buildings has not been adequately investigated yet. HP has been considered an expensive technology for environmental control in animal housing compared with conventional technologies. The recent advancements in HP's technology, though, have led to considerable improvement in the coefficient of performance (COP), making the technology worthy of further investigation. Furthermore, their coupling with other renewable energy sources (RES) systems (i.e., photovoltaic and geothermal energy systems) not only can improve HP systems' performance but also assist in the energy resilience of the facilities during periods of energy uncertainty. The successful integration and adoption of HPs in broiler houses could considerably benefit EU livestock facilities in the near future. HPs are considered an RES technology, closely following the European Commission (EC) priorities on energy efficiency [25], and are fully in line with

the new strict EU directives for energy performance in buildings which require reaching nearly zero energy buildings (nZEBs) status [26] in the short term.

The present study follows the preliminary work of Tyris et al. [27], where the dynamic operation of modular HPs regulating the indoor climate of a broiler house was simulated for two production periods (PPs). Here, a more sophisticated model of the heat pump system is developed. First, two widely used technologies are incorporated, namely, a heat recovery system and an evaporative cooling pads system. Furthermore, seven PPs—instead of two—are simulated, while exhaustive results on energy use and operation time per mode for two scenarios—with and without evaporative cooling pads—are elaborated. Except for the accurate modeling of the HP's components and operation, the novelty of our study lies in the introduction of a modular HP as the main HVAC system regulating the indoor environment of a broiler house. This was identified as the first step towards investigating the application of this recently ascendant technology in the intensive livestock farming industry. The model developed in this study is capable of (i) simulating the indoor environment conditions, and (ii) estimating the heating, cooling, and dehumidifying loads and energy use of the HVAC system, thus providing insight into its performance for practical implementation purposes.

The seven different PPs during a typical meteorological year are considered to evaluate the annual total electrical energy consumption. The study shows an annual energy use of 80,506.0 kWh, or 129.4 kWh/m², with dehumidifying and cooling needs being dominant throughout the year and exceeding the heating needs. In terms of efficiency, the seasonal COP (SCOP) factor was estimated for heating and dehumidifying, and the seasonal energy efficiency ratio (SEER) was estimated for cooling. SCOP can reach above 3.1 and 4.8 for heating and dehumidifying, respectively, while SEER for cooling is above 3.7.

The present study aims to fill the gap found in the literature concerning the investigation of HP technology in livestock environments by introducing detailed modeling of its operation in a broiler house environment. It is expected that the findings of the present work may assist in the adoption of HVAC systems with HP in the sector of livestock buildings, leading to more efficient energy use.

2. Modeling and Analysis

In the present study, a mathematical model is developed in the MathWorks Simulink/Simscape environment [28,29] to simulate the thermal loads of a broiler house and the dynamic operation of a modular HP system. The broiler house was modeled as an open thermodynamic system within which a controlled exchange of energy and mass takes place. The modeled HP system aims at covering the heating, cooling, and dehumidifying needs of the facility. The model takes into consideration both the internal and the external heat loads to (i) accurately predict the real-time internal conditions of the house, and (ii) efficiently operate the HVAC system to create indoor conditions for optimal broiler growth. The internal heat loads are affected by the number of broilers and their growth stage, as their mass affects both their sensible and latent heat loads. On the other hand, the external heat loads depend on the local climatic data and the considered heat transfer mechanisms. This study considers all the heat transfer mechanisms, namely, (i) solar radiation to the roofs and external walls, (ii) convection between the outside wall and the external air, (iii) conduction through the construction materials, and (iv) convection between the inside wall and the internal air. Finally, the energy use of all HP modes, as well as the overall energy consumption, are estimated and the appropriate energy efficiency indicators (SCOP and SEER) are calculated. The flow diagram of the numerical model is presented in Figure 1.

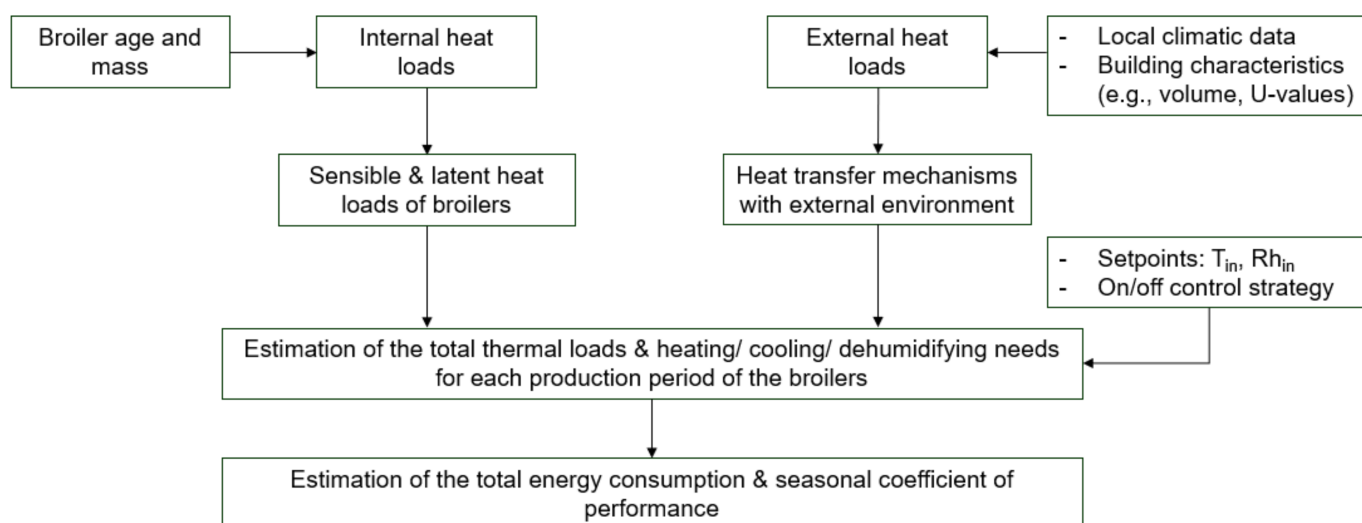


Figure 1. Flow diagram of the numerical model.

The dynamic simulations performed offer a full understanding of the broilers' interaction with the environment, leading to the definition of heat balances and the heating, cooling, and dehumidifying requirements.

2.1. Broilers and Building Envelope

A total of 10,000 broilers are housed per PP in the simulated facility located in northern Greece (Kavala area; 40.94° N, 24.41° E), with a humid climate, cold winters, and hot summers. Values of the outdoor temperatures and relative humidities of a typical meteorological year were used, while solar radiation was calculated [30]. Soil temperature at a depth of 50 cm ($T_{gr,0.50}$) was correlated to outside air temperature ($T_{out-air}$) using functions (Equations (1) and (2)) developed for northern Greece [31]:

$$T_{gr,0.50} = -0.0116 \cdot T_{out-air}^2 + 1.4289 \cdot T_{out-air} - 0.3515 \quad (\text{from August to January}) \quad (1)$$

$$T_{gr,0.50} = 0.0116 \cdot T_{out-air}^2 + 0.6737 \cdot T_{out-air} + 3.0285 \quad (\text{from February to July}) \quad (2)$$

For the modeling of walls and roofs, the thermal transmittance (U-value) for a 4 cm polyurethane panel was used, providing a value very similar to commercial products [32]. The floor's U-value was estimated for a floor structure consisting of 15 cm of concrete, 8 cm of sawdust litter, a 2 cm waterproofing layer, a 2 cm concrete coating, and 25 cm of soil. Table 1 summarizes the main building's characteristics used for this work.

Table 1. Broiler house dimensions and envelope characteristics ¹.

	Value	Units
Length	45.70	[m]
Width	13.61	[m]
Gutter height	3.55	[m]
Roof inclination	9.00	[deg]
Area	622.00	[m ²]
Volume	2419.00	[m ³]
U_{walls}, U_{roof} ²	0.57	[W/m ² K]
U_{floor}	0.52	[W/m ² K]

¹ Adapted from Manolakos et al. [33]. ² Thermal transmittance (U-value).

In general, modern broiler houses are characterized by simplicity in construction (i.e., single room, polyurethane/metal sheet walls, airtight, no considerable major machinery, etc.). Even though these buildings are classified as "lightweight" constructions [34], the

building's thermal mass has been included and considered as a model input. The simulation's results are presented for seven possible PPs, 35 days each, throughout the course of a year, with varying ambient temperature and relative humidity. The PPs that were considered for this study are presented in Table 2. The potential influence of a shift in the PPs' dates on the overall energy consumption could be investigated in a future study.

Table 2. Simulated production periods (PPs).

Production Period (PP)	Start Date	End Date	Temperature [°C] min./max./avg.	Humidity [%] min./max./avg.
1	1st January	5th February	−5.90/14.80/4.01	37.60/99.50/80.08
2	20th February	27th March	−4.60/19.90/8.25	31.80/98.70/68.99
3	11th April	16th May	3.70/23.00/13.75	32.90/97.90/70.28
4	31st May	5th July	14.00/32.80/23.50	29.60/86.80/60.91
5	20th July	24th August	18.80/34.20/25.62	19.60/80.40/51.80
6	8th September	13th October	12.40/29.60/19.87	22.40/92.70/60.45
7	28th October	2nd December	4.80/20.20/14.25	43.50/94.20/76.40

The broiler houses are characterized by broadly varying thermal loads because of the fast growth rate and the increased population density. The recommended temperature setpoint and relative humidity limits are a function of broiler age [35]. The broilers' mass, m_{br} (kg), at each day within a PP is given by Equation (3) below [36]:

$$m_{br} = f_1 \cdot d^3 + f_2 \cdot d^2 + f_3 \cdot d + f_4 \quad (3)$$

The values for factors f_i , $i = 1 \dots 4$ are given in Table 3, while the broilers' mass during a PP is presented in Figure 2a, reaching up to 2.2 kg on the final day of each period.

Table 3. Factors for broiler mass calculation.

Factor	Value	Units
f_1	-2.1164×10^{-5}	[kg/day ³]
f_2	$+2.5608 \times 10^{-3}$	[kg/day ²]
f_3	-5.3002×10^{-3}	[kg/day]
f_4	$+7.0839 \times 10^{-2}$	[kg]

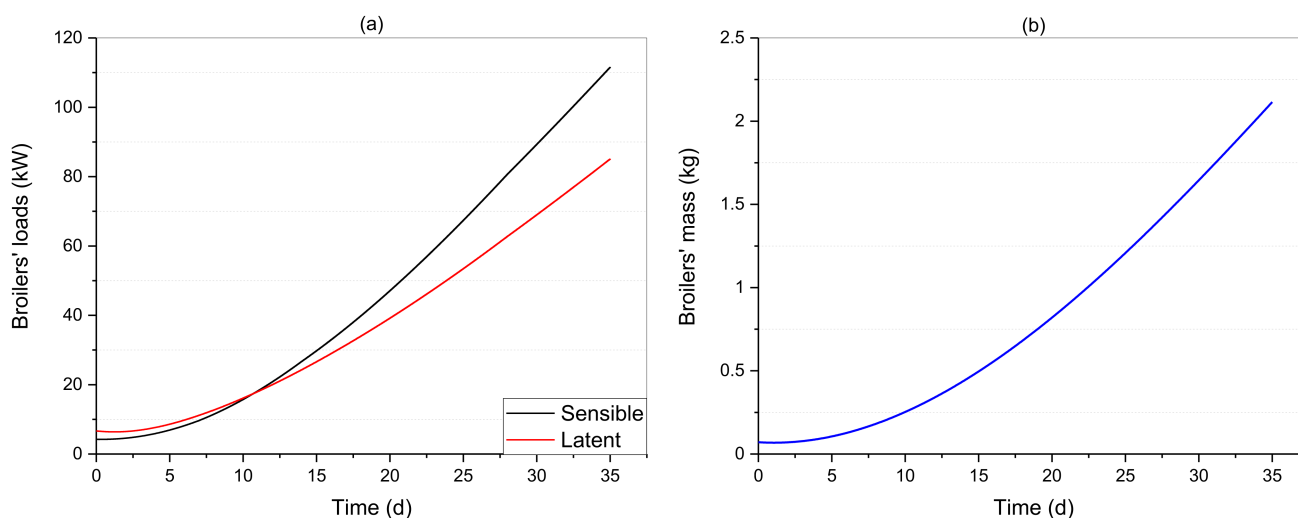


Figure 2. Increase in (a) broilers' sensible and latent thermal loads of the flock and (b) mass during a 35-day production period (PP).

In Figure 2b, besides the increase in cooling needs, as the broilers' mass increases, a significant increase in latent heat is indicated. Between the 20th and 35th day of the PP, the latent loads are more than doubled, going from 39.2 to 85.1 kW (117% increase).

A common management practice in broiler housing is to restrict the flock to one-third, or one-half, of the building area until the 10th day. In the current model, the entire available floor area was used to house the flock in order to simplify the envelope modeling process in Simulink. Consequently, the necessary thermal loads over this period are overestimated to some extent.

2.2. Heat Loads

2.2.1. Internal Heat Loads

For simplicity, the internal space of the broiler house was considered free of equipment and appliances (e.g., feeders, waterers, mixing fans, etc.). As a result, the internal heat load is restricted to the broiler heat loads. Practically, the broiler mass can be considered as a heat source of polynomial varying magnitude (Equation (3)). For the calculation of the heat produced by the broilers, the methodology followed by Manolakos et al. [33] was also adopted in the current study.

Usually, it is practical to refer to the specific heat production unit (*hpu*) Φ_{tot} (1000 W of animal total heat production) at an ambient temperature of 20 °C [37]. For lower or higher temperatures, *hpu* is adjusted, $\Phi_{tot-1000}^*$ (W), according to Equation (4):

$$\Phi_{tot-1000}^* = 1000 \cdot [1 + 4 \cdot 10^{-5} \cdot (20 - T_{rm})^3] \quad (4)$$

For broilers housed between 10 °C and 40 °C, the corresponding sensible heat production at house level, Φ_{s-1000}^* (W), is given by Equation (5):

$$\Phi_{s-1000}^* = 805 - 39.216 \cdot T_{rm} + 2.2288 T_{rm}^2 - 0.0438 T_{rm}^3 \quad (5)$$

The ratio of sensible to total heat production is given by Equation (6). When combined with Equations (7)–(10), the heat loads of broilers can more accurately be estimated:

$$r = \frac{\Phi_{s-1000}^*}{\Phi_{tot-1000}^*} \quad (6)$$

$$\Phi_{tot} = N \cdot 10 \cdot m_{br}^{0.75} \quad (7)$$

$$\Phi_{tot-1000}^* = 1000 \cdot [1 + 4 \times 10^{-5} \cdot (20 - T_{rm})^3] \quad (8)$$

$$\Phi_{tot-sen}^* = r \cdot \Phi_{tot}^* \quad (9)$$

$$\Phi_{tot-lat}^* = \Phi_{tot}^* - \Phi_{tot-sen}^* \quad (10)$$

In the above equations, T_{rm} is the broiler house temperature, N is the number of broilers in the house, and m_{br} (kg) is the mass of each broiler. The heat produced by litter (60% sensible, and 40% latent) was also considered, accounting for 10% of the total heat produced by broilers [38]. As breeding days go by, heat loads from litter increase, thus increasing the need for cooling and dehumidifying. Figure 3 illustrates the variation of the broilers' total heat loads during the 35 days for each PP. It is worth noticing that the thermal load for each period increases significantly, beginning from 12 kW and reaching up to 200 kW at the end of the period.

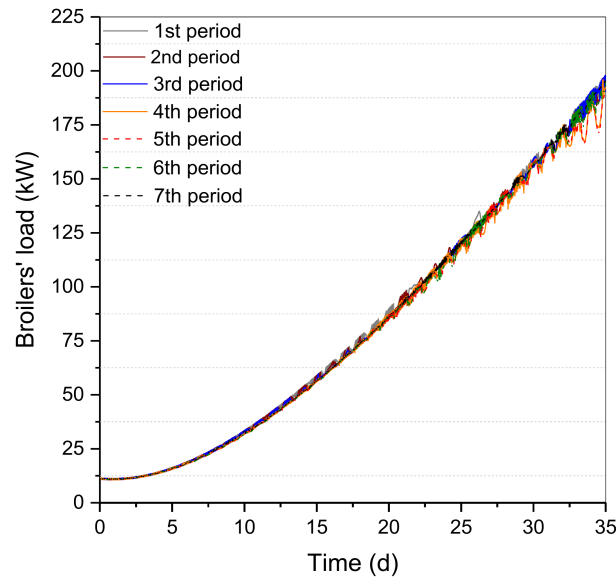


Figure 3. Broilers' thermal loads increase during each PP.

2.2.2. External Heat Loads

In the case of a modern broiler house, only walls, roof, and floor are considered since no windows, partitions, skylights, or other structures exist. For the calculation of sensible heat flow through the external opaque surfaces of the building, the heat transfer mechanism considered is a combined convection–conduction type, $Q_i^{conv-cond}$ (W), shown in Equation (11), with the addition of the solar radiation incident to each surface i , Q_i^{rad} (W):

$$Q_i^{conv-cond} = U \cdot A_i \cdot (T_i - T_{rm}) \quad (11)$$

where U (W/m²K) is the overall heat transfer coefficient, A_i (m²) is the area of the surface i , and T_i (°C) is the temperature of the wall. Since the envelope has been considered airtight, the mass transfer takes place by mechanical ventilation, which is necessary for carbon dioxide concentration control. Its minimum volumetric rate (m³/s) is indicated in Equation (12) (adapted from [37]):

$$\dot{V}_{air-CO_2} = \frac{v_i \cdot \dot{m}_{air-CO_2}}{[CO_{2i}] - [CO_{2o}]} \quad (12)$$

where v_i (m³/kg) is the specific volume of the inside air, \dot{m}_{air-CO_2} (kg/s) is the mass flow rate of the air, $[CO_{2i}]$ (ppm) is the maximum (3000 ppm) allowable carbon dioxide concentration of the inside air, and $[CO_{2o}]$ (ppm) is the average (385 ppm) carbon dioxide concentration of the outside air. The sensible and latent heat flow (W) due to ventilation are given by Equations (13) and (14), respectively [39]:

$$\dot{Q}_{OASH} = 1.23 \cdot \dot{V}_{air-CO_2} \cdot (T_{out-air} - T_{rm}) \cdot 10^3 \quad (13)$$

$$\dot{Q}_{OALH} = 3010 \cdot \dot{V}_{air-CO_2} \cdot (\omega_{out-air} - \omega_{rm}) \cdot 10^3 \quad (14)$$

$\omega_{out-air}$ (kg of water/kg of dry air) and ω_{rm} (kg of water/kg of dry air) is the absolute humidity of outside air and room, respectively, representing the ratio of water mass to dry air mass.

2.3. Heat Pump Model

An HVAC system should effectively cover heating and cooling loads, reassuring the minimum required ventilation while maintaining the relative humidity at acceptable levels. The HP system was simulated as a dynamic model using the commercial software Simulink

to cover the heating, cooling, and dehumidifying needs of the building. The three HPs were modeled as air-cooled units, while R134a refrigerant was employed as the working fluid.

The HPs regulate their operation to reach the desired setpoint for the indoor temperature, while the relative humidity also needs to be kept within acceptable limits to ensure welfare conditions for the broilers. Three HPs for heating, cooling, and dehumidifying have been employed in the developed model. The heating mode is enabled when the indoor temperature drops 2 °C below the setpoint and deactivated when the setpoint is reached. Cooling is activated when a temperature difference of 2 °C between indoor and setpoint temperatures emerges. In case this difference increases beyond 3 °C, a second cooling module is activated, while both are deactivated when the setpoint temperature is achieved. To reduce the energy use of the cooling mode, when the outdoor temperature is lower relative to the indoor one, the outdoor air is utilized as a cooling source (free cooling mode).

Similarly, in the case of relative humidity regulation, three dehumidification modules are enabled, while for each mode a reheating coil is enabled to avoid over-cooling of the supplied dehumidified air. The operation is activated for each dehumidification mode when a +1%, +2%, and +3% difference in relative humidity between the inside and fresh air emerges, respectively.

Additionally, when the relative humidity drops below the lower limit, an auxiliary humidifier, with a mass flow rate of 10 kg/h, is put into operation. To enhance the system performance, an air-to-air recuperator with a total heat exchange area of 500 m² and heat transfer coefficient of 25 W/m²K is also incorporated to recover the heat of the exhaust air preheating the fresh air that enters the room.

The developed model utilized Simscape blocks available in the Simulink environment. By connecting these blocks, multidomain physical systems were assembled to model the building environment, as well as the heat pump system. The function of the blocks of these libraries is based on formulas considering dynamics, such as the variation of heat and pressure losses with temperature and mass flow rates. The main Simscape blocks used to construct the necessary physical networks for simulating the heat pump's operation are: (i) condenser evaporator, (ii) thermostatic expansion valve, (iii) pipe, (iv) controlled reservoir, (v) constant chamber volume, and (vi) controlled mass flow rate source. The above, combined with several auxiliary blocks, resulted in satisfactory modeling of the heat pumps' dynamic operation.

The Simscape libraries used are the Moist Air (MA) [40], Two-Phase (2P) Fluid [41], and Thermal Liquid (TL) [42].

Main Components

The selected compressor is a Bitzer 6GE-34Y semi-hermetic reciprocating compressor [43] operating with an inverter to control its frequency, a displacement of 126.8 m³/h at 1450 rpm, and a volume ratio of 3. Its mass flow rate (kg/h) and the power consumption (W) were calculated based on the polynomial coefficients (Equation (15)) provided by the manufacturer [44]. The polynomials are a function of the evaporation (T_{ev}) and condensation (T_{cd}) temperatures and the mass flow rate and power consumption coefficients ($c_1, c_2, \dots, c_9, c_{10}$) at different compressor frequencies. The mass flow and power consumption coefficients used can be found in Tables A1 and A2 of the Appendix A, respectively.

$$y = c_1 + c_2 \cdot T_{ev} + c_3 \cdot T_{cd} + c_4 \cdot T_{ev}^2 + c_5 \cdot T_{ev} \cdot T_{cd} + c_6 \cdot T_{cd}^2 + c_7 \cdot T_{ev}^3 + c_8 \cdot T_{cd} \cdot T_{ev}^2 + c_9 \cdot T_{ev} \cdot T_{cd}^2 + c_{10} \cdot T_{cd}^3 \quad (15)$$

The condenser and evaporator of the HP were modeled as plate-fin heat exchangers with crossflow, employing the Condenser-Evaporator (TL-MA) Simscape block, where heat is exchanged between the refrigerant and moist air. The appropriate flow and geometrical characteristics are set to reflect the problem specifications. Heat transfer between the indoor/outdoor air and refrigerant is calculated based on the effectiveness–number of transfer units (ϵ -NTU) method, where the Gnielinski correlation is used for the subcooled liquid or superheated vapor zones and the Cavallini-Zecchin correlation is used for the

liquid–vapor mixture zone. The condenser has a total fin surface area of 420.2 m², while the evaporator surface area is 226.9 m². The condenser and evaporator heat transfer characteristics are presented in Table 4.

Table 4. Characteristics of evaporator and condenser.

Parameter	Condenser	Evaporator
Heat transfer coef. (W/m ² K)	5.3	32.8
Heat transfer area (m ²)	420.2	226.9

Finally, a thermostatic expansion valve, moderating the refrigerant flow, was modeled using the thermostatic expansion valve (2 P) Simscape block. The opening of the valve was adjusted to achieve the desired superheat at the evaporator outlet (5 K).

The model estimated the *COP* and *EER* of the heating and cooling capacity of the heat pump, respectively, taking into consideration the power consumed by the compressor for the rejected and provided heat, as shown in Equations (16) and (17):

$$COP = \frac{\dot{Q}_{heat}}{\dot{W}_{comp}} \quad (16)$$

$$EER = \frac{\dot{Q}_{cooling}}{\dot{W}_{comp}} \quad (17)$$

For validation purposes, the results of the developed HP model were compared with those of the software provided by the compressor manufacturer [44]. The deviations of heating capacity and *COP* for steady operation at various operating points were calculated based on Equation (18):

$$D = \frac{M - S}{S} \cdot 100\% \quad (18)$$

In the above equation, *D* is the deviation (%), and *M* and *S* are the results of the model and manufacturer's software, respectively. Figure 4 presents the variation between the developed model and the expected performance from the compressor's manufacturer, showing a deviation below 2%. Therefore, the heat pump model is considered to present acceptable accuracy in predicting the whole system operation, presenting similar results for the heating capacity and *COP*.

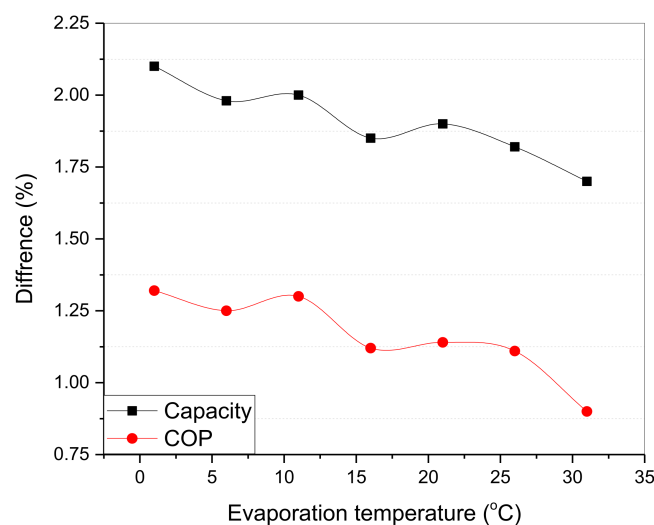


Figure 4. Variation of capacity and coefficient of performance (*COP*) between the developed model and the expected compressor's performance.

3. Results and Discussion

Considering the external conditions (temperature, relative humidity, and solar radiation) and internal loads, the HP system provides the necessary heating, cooling, and dehumidifying loads to maintain the broilers' house temperature and relative humidity within the acceptable range. As explained above, the HPs turn on and off their operation depending on the temperature and humidity differentials, leading to fluctuating conditions. The indoor temperature and relative humidity profiles that resulted from simulating the HPs' operation for the seven PPs are presented next.

3.1. Indoor Temperature and Relative Humidity

The variation of indoor temperature and relative humidity during the 1st PP (01.01–05.02) is shown in Figure 5. Outdoor temperature ranges between -5.90 and 14.8 °C (avg. 4.01 °C) and relative humidity between 37.6 and 99.5% (avg. 80.1%). The indoor temperature presents a maximum deviation of -2.5 °C from the setpoint, during the first 20 days, and approximately $+2.1$ °C during the last 5 days, when the outdoor temperature increases. The indoor relative humidity falls within the acceptable limits, exceeding the upper one by about $+2.2\%$, only during the last 5 days of the PP.

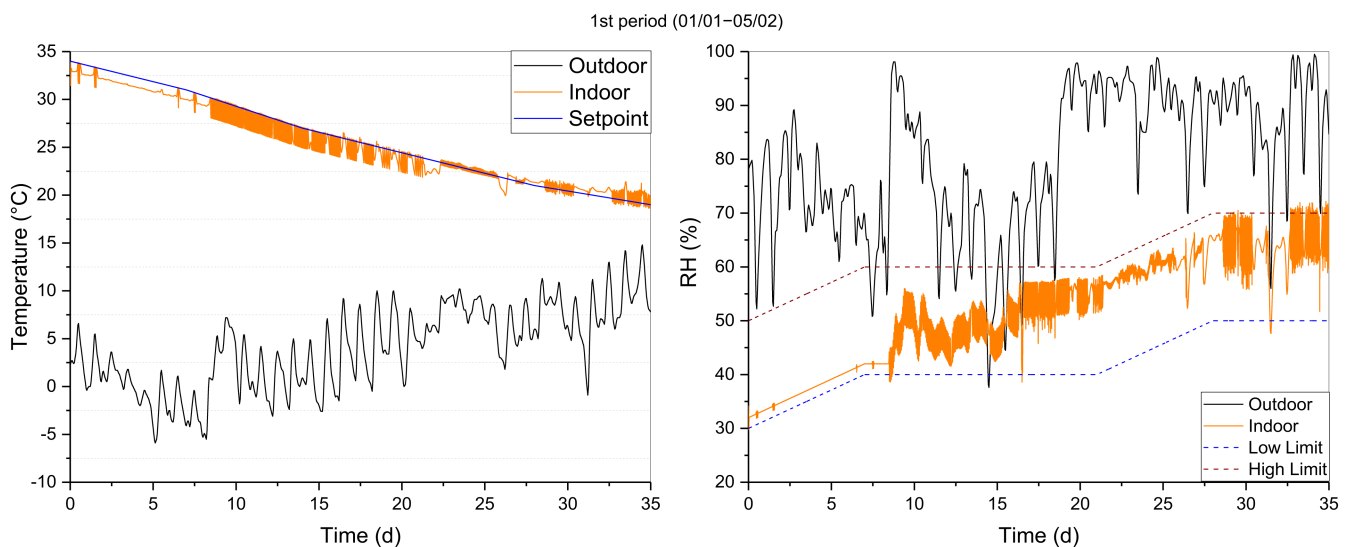


Figure 5. Temperatures and relative humidity variation during the 1st production period (01.01–05.02).

The variation of indoor temperature and relative humidity during the 2nd PP (20.02–27.03) is presented in Figure 6. The outdoor temperature ranges between -4.60 and 19.9 °C (avg. 8.25 °C) and relative humidity between 31.8 and 98.7% (avg. 69.0%). For the largest part of the PP2, the indoor temperature presents a maximum deviation of $-2.5/+2.1$ °C. Except for temporary deviations (max. -13.2%), the relative humidity stays within the acceptable range.

During the 3rd PP (11.04–16.05), the outdoor temperature ranges between 3.7 and 23.0 °C (avg. 13.8 °C), and relative humidity between 32.9 and 97.9% (avg. 70.3%). The indoor temperature (max. deviation: $-2.4/+3.0$ °C) and relative humidity (max. deviation: $-12.0/+2.9$ °C) show a behavior similar to the 2nd PP (Figure 7).

The variation of indoor temperature and relative humidity during the 4th PP (31.05–05.07) is shown in Figure 8. The outdoor temperature ranges between 14.0 and 32.8 °C (avg. 23.5 °C) and relative humidity between 29.6 and 86.8% (avg. 60.9%). A maximum deviation ($+5$ °C) between the indoor temperature and the setpoint during the last 2 days can be observed. The HP does not seem capable of covering the cooling needs of these two days. The deviation is caused by the high outdoor temperature during this period, in combination with the broilers' size, which leads to increased thermal loads and high ventilation

needs. Finally, the relative humidity only temporarily deviates from the acceptable range ($-2.2/+3.1\%$).

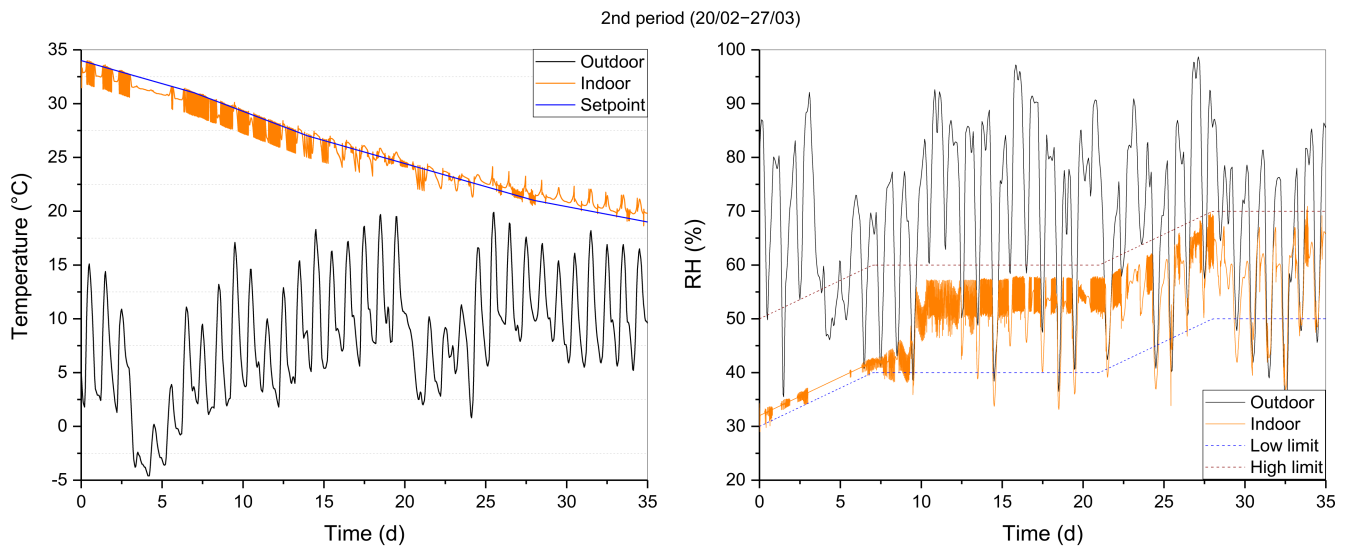


Figure 6. Temperatures and relative humidity variation during the 2nd production period (20.02–27.03).

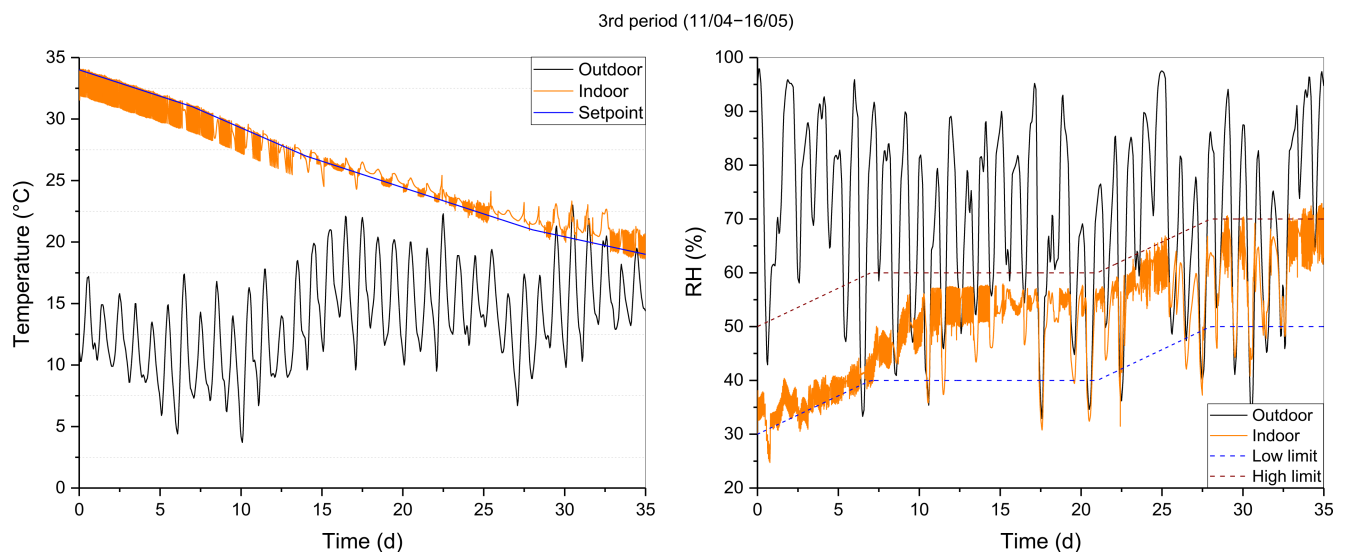


Figure 7. Temperatures and relative humidity variation during the 3rd production period (11.04–16.05).

During the 5th PP (20.07–24.08) outdoor temperature ranges from 18.8 to 34.2 °C (avg. 25.6 °C) and relative humidity from 19.6 to 80.4% (avg. 51.8%). Indoor conditions exhibit a behavior similar to the 4th PP, with temperature deviating between -2.3 and $+5.7$ °C, and relative humidity between -5.9 and $+1.5\%$ (Figure 9).

In the course of the 6th PP (08.09–13.10), outdoor temperature ranges from 18.8 to 34.2 °C (avg. 25.6 °C) and relative humidity from 19.6 to 80.4% (avg. 51.8%). Even though the indoor temperature profile follows a pattern similar to PP5, with maximum deviations of -2.3 and $+3.1$ °C, the deviations from the acceptable range in the case of humidity are greater (Figure 10). A -18.1% deviation was observed twice during the first 6 days.

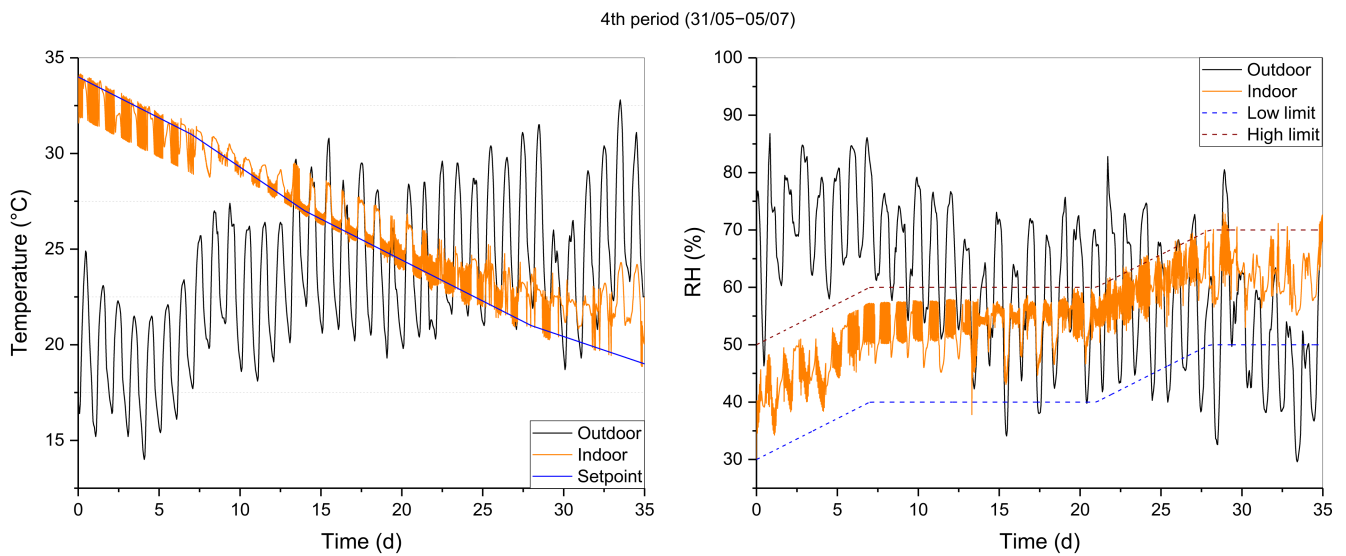


Figure 8. Temperatures and relative humidity variation during the 4th production period (31.05–05.07).

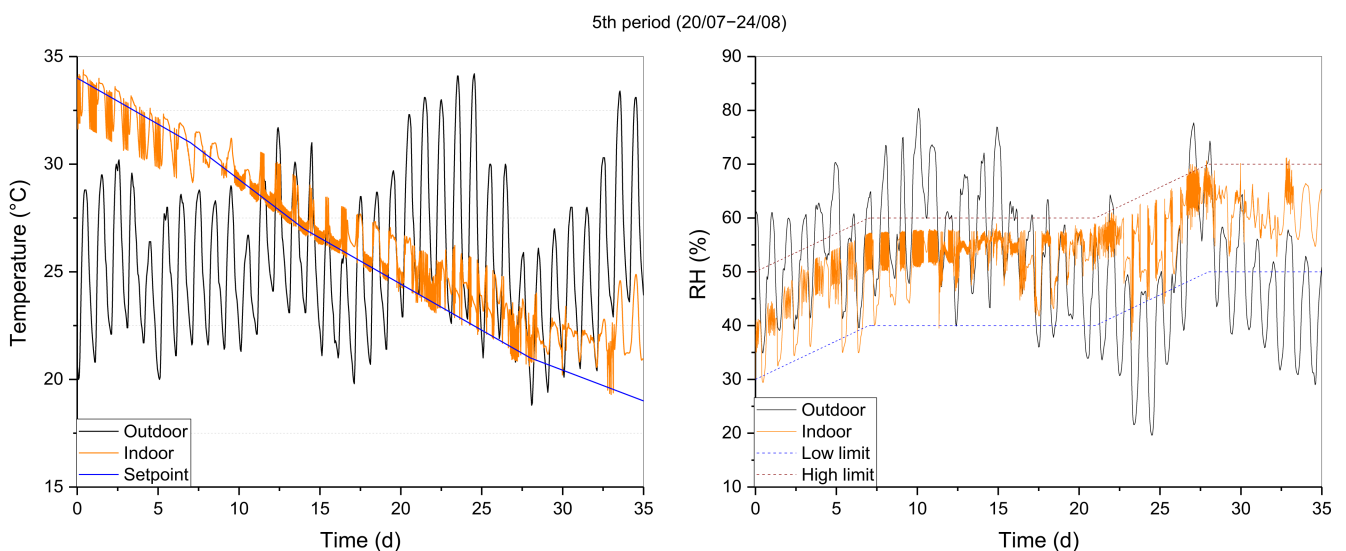


Figure 9. Temperatures and relative humidity variation during the 5th production period (20.07–24.08).

Finally, during the 7th PP (28.10–02.12), the outdoor temperature ranges from 4.8 to 20.2 °C (avg. 14.3 °C), and relative humidity from 43.5 to 94.2% (avg. 76.4%). The indoor conditions' profile is similar to those of PP1 and PP2 (Figure 11). A deviation of $-2.3/ +2.0$ °C for the setpoint is observed in the case of temperature. Concerning relative humidity, a $-5.5/ +0.8$ % deviation is noticed.

Due to the dynamic nature of the model, the HP's response is influenced by both the outdoor and desired indoor conditions. Principally, the modeled HP system appears capable of covering the broiler house's necessary loads, with the likely exception of cooling loads, mostly during PP4 and PP5. These fluctuations are considered insignificant during a whole year; therefore, extra modes that would increase the broiler's house operating costs have not been considered. The observed fluctuations and overshoot in both temperature and relative humidity will be further discussed in Section 3.3 ("Control aspects").

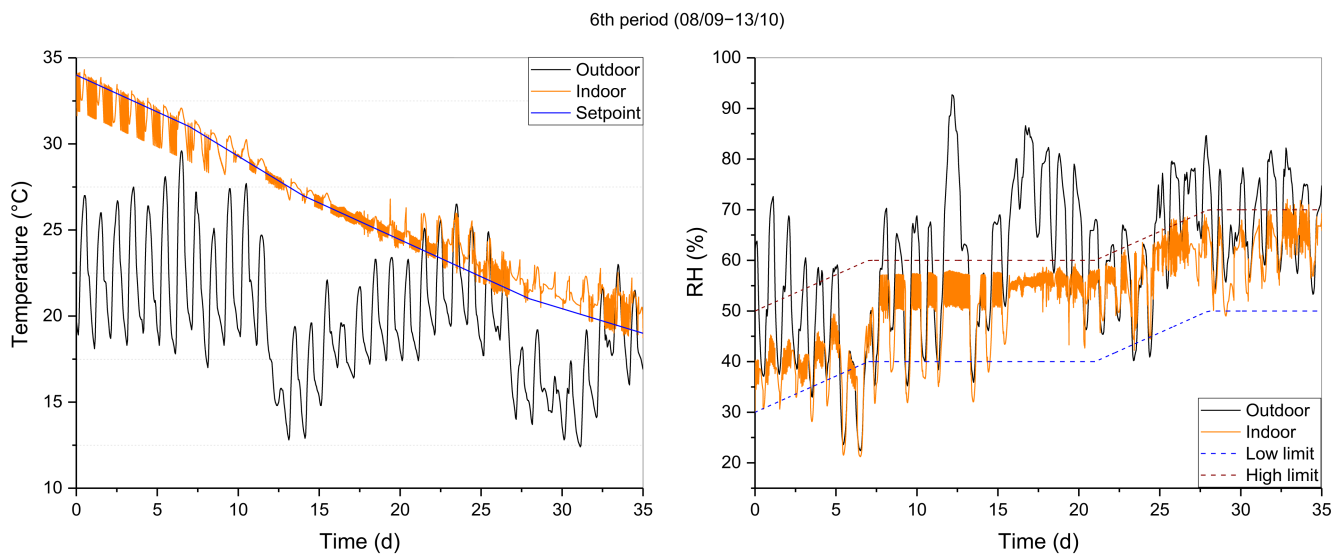


Figure 10. Temperatures and relative humidity variation during the 6th production period (08.09–13.10).

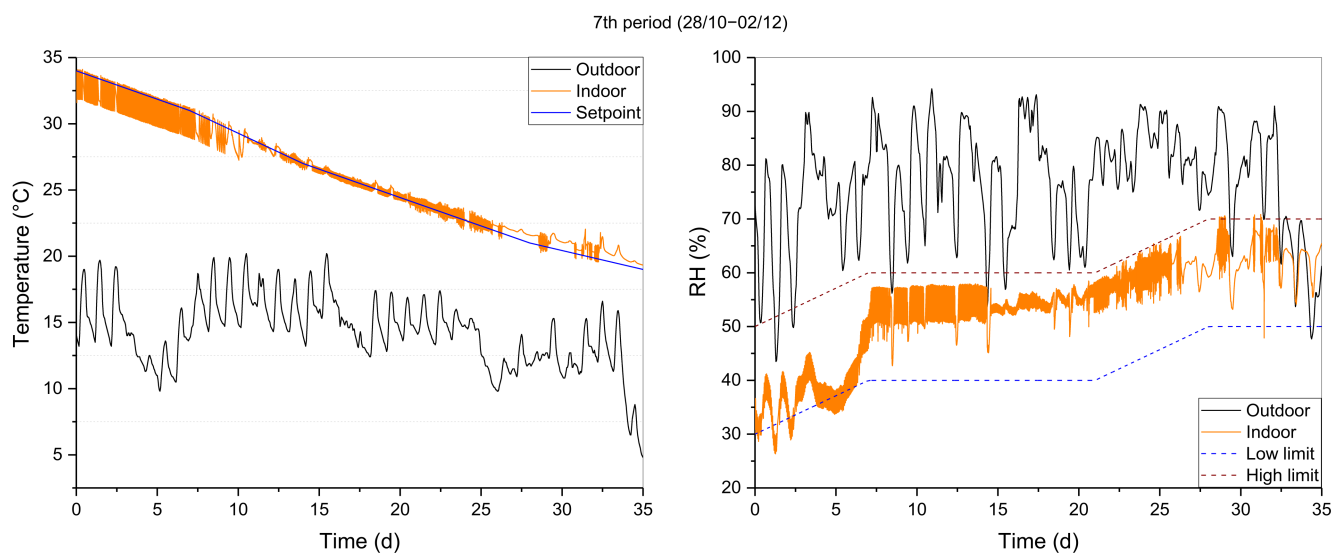


Figure 11. Temperatures and relative humidity variation during the 7th production period (28.10–02.12).

3.2. Energy Use

For all PPs, the energy use (kWh) of each HP's mode, energy use per square meter (kWh/m²), as well as operation time (h) are presented in Table 5. Additionally, seasonal energy efficiency indicators for each mode were also calculated. These are the SCOP for heating and dehumidifying and SEER for cooling, which are largely dependent on ambient (outdoor) temperature and the required indoor conditions. When more than one module of the same mode is employed, an average value is estimated.

The overall energy use is calculated at 80,506.0 kWh, or 129.4 kWh/m², yearly. PP4 and PP5 appear to be the most energy-intensive periods, with 19,745.8 kWh and 18,359.8 kWh, respectively, mainly due to the increased cooling needs. Cooling is higher during PP5 (11,884.5 kWh), while dehumidifying is higher during PP4 (8859.0 kWh). Concerning the cooling mode, SEER ranges from 7.0 (PP7) to 3.7 (PP4), largely depending on the outdoor temperature. Similarly, dehumidifying mode's SCOP ranges from 7.9 (PP2) to 4.8 (PP4). In terms of heating, PP1 is the most demanding, followed by PP2 and PP3. The heating mode's SCOP does not vary considerably, ranging from 3.5 to 3.1, showing that the HP

performance is improved when the ambient temperature is higher. Free cooling and CO₂ ventilation energy use are more or less the same throughout the year. It is worth mentioning that, in addition to the operation of HP, the humidifier consumes a total of 5194.3 kg of water during 973.2 h of operation.

Table 5. Energy use and energy efficiency indicators of each operation mode per production period.

Production Period (PP)	Operation Mode	Energy Use [kWh]	Energy Use per m ² [kWh/m ²]	Operation Time [h]	Average SCOP/SEER
1 (01.01–05.02)	Heating	4378.2	7	272.4	3.1
	Cooling	36.1	0.1	3.4	5.9
	Dehumidifying	3607.5	5.8	301.8	7
	Free cooling	133.2	0.2	151.1	-
	CO ₂ Ventilation	384.3	0.6	436	-
	TOTAL	8539.3	13.7	-	-
2 (20.02–27.03)	Heating	3018.5	4.9	170.3	3.1
	Cooling	671.5	1.1	79.5	6.4
	Dehumidifying	1549.8	2.5	135.4	7.9
	Free cooling	349.5	0.6	320.4	-
	CO ₂ Ventilation	382.5	0.6	350.6	-
	TOTAL	5971.8	9.6	-	-
3 (11.04–16.05)	Heating	1762.2	2.8	64.5	3.2
	Cooling	1509.1	2.4	110.7	5
	Dehumidifying	4932	7.9	334.5	5.6
	Free cooling	478.3	0.8	366	-
	CO ₂ Ventilation	381.1	0.6	291.6	-
	TOTAL	9062.7	14.6	-	-
4 (31.05–05.07)	Heating	539.7	0.9	17.9	3.4
	Cooling	9596.7	15.4	398.8	3.7
	Dehumidifying	8859	14.2	522.2	4.8
	Free cooling	371.8	0.6	205.1	-
	CO ₂ Ventilation	378.5	0.6	208.7	-
	TOTAL	19,745.8	31.7	-	-
5 (20.07–24.08)	Heating	191	0.3	6.3	3.5
	Cooling	11,884.5	19.1	525.2	3.7
	Dehumidifying	5377.9	8.6	328.8	4.8
	Free cooling	528.9	0.9	302.9	-
	CO ₂ Ventilation	377.6	0.6	216.2	-
	TOTAL	18,359.8	29.5	-	-
6 (08.09–13.10)	Heating	382.1	0.6	12.6	3.4
	Cooling	2806	4.5	172.9	4.6
	Dehumidifying	6561.3	10.5	405.2	5.1
	Free cooling	669	1.1	435.8	-
	CO ₂ Ventilation	379.7	0.6	247.3	-
	TOTAL	10,798.2	17.4	-	-
7 (28.10–02.12)	Heating	1236.1	2	42.5	3.3
	Cooling	507	0.8	66.4	7
	Dehumidifying	5627.6	9	388.9	6.2
	Free cooling	276.3	0.4	270.6	-
	CO ₂ Ventilation	381.5	0.6	373.6	-
	TOTAL	8028.5	12.9	-	-

As shown in Table 6, dehumidifying is the most energy-consuming HP mode year-round (36,515.1 kWh), followed by cooling (27,010.9 kWh). It must be noted that the energy use data provided above also include the operation of reheating. The dehumidifying to reheating load ratio varies depending on the needs of each PP, ranging from 2.81 (PP2) to

7.28 (PP5). Heating (11,507.8 kWh) comes third, with less than half of the cooling's energy use, since, for a significant period, the broiler's thermal load covers a large percentage of the heating needs. Free cooling and CO₂ ventilation present comparable energy use (2807.0 and 2665.1 kWh, respectively). A total average daily energy use is calculated at 2300.2 kWh, yearly, while the total energy use per m² is 129.4 kWh/m².

Table 6. Total energy use and average energy efficiency indicators yearly.

Operation Mode	Energy Use [kWh]	Operation Time [h]	Energy Use per m ² [kWh/m ²]	Average Daily Energy Use [kWh]	Average SCOP/SEER
Heating	11,507.8	586.5	18.5	328.8	3.3
Cooling	27,010.9	1356.8	43.4	771.7	5.2
Dehumidifying	36,515.1	2416.9	58.7	1043.3	5.9
Free cooling	2807.0	2051.8	4.5	80.2	-
CO ₂ Ventilation	2665.1	2124	4.3	76.1	-
TOTAL	80,506.0	-	129.4	2300.2	-

Two facts render the comparison of the obtained results with recent literature difficult. First, there is no available energy use data, simulated or real, for HPs incorporated in broiler houses. Second, as discussed in Section 1, there is a gap in the study of energy use data in general [15] and consequently for energy use climate control. The total energy consumption per m² in Table 6 refers to the regulation of the indoor environment undertaking a fully featured approach, using different operation modes of HP. Since there are no similar data available, only the thermal energy provided for heating can be used as a reference point. As shown in Table 7, the obtained results for year-round heating (58.7 kWh/m²) are comparable to the ranges found in [16,17]:

Table 7. Comparison of simulated thermal energy use for heating with literature data.

Study	Thermal Energy per m ² [kWh/m ²]
Current study	58.7
M. de Vries and I. J. M. de Boer [16]	60–80
Costantino et al. [17]	86–137

3.3. Incorporation of Evaporative Cooling Pads

Since the overall cooling needs have been determined to be considerably high, the investigation of the performance of a system incorporating evaporative cooling pads was also considered. Evaporative cooling is a conventional cooling selection using air's enthalpy to vaporize water, resulting in a reduced air temperature and increased humidity. These systems constitute a common practice in poultry houses, especially during summer months, due to their low operational costs. For our purposes, evaporative pads with a saturation efficiency of 75% were incorporated into the model for the 4th and 5th PP, which present the highest cooling requirements.

Compared with the simulations without evaporative cooling pads, the results for PP4 present similar temperature deviation (Figure 12), while relative humidity is slightly improved, deviating from −0.0 to +3.1%. Finally, in PP5 (Figure 13), temperature deviation shows no difference compared with the system without pads, while relative humidity (−0.0 to +1.7%) is improved (−5.9 to +1.5%).

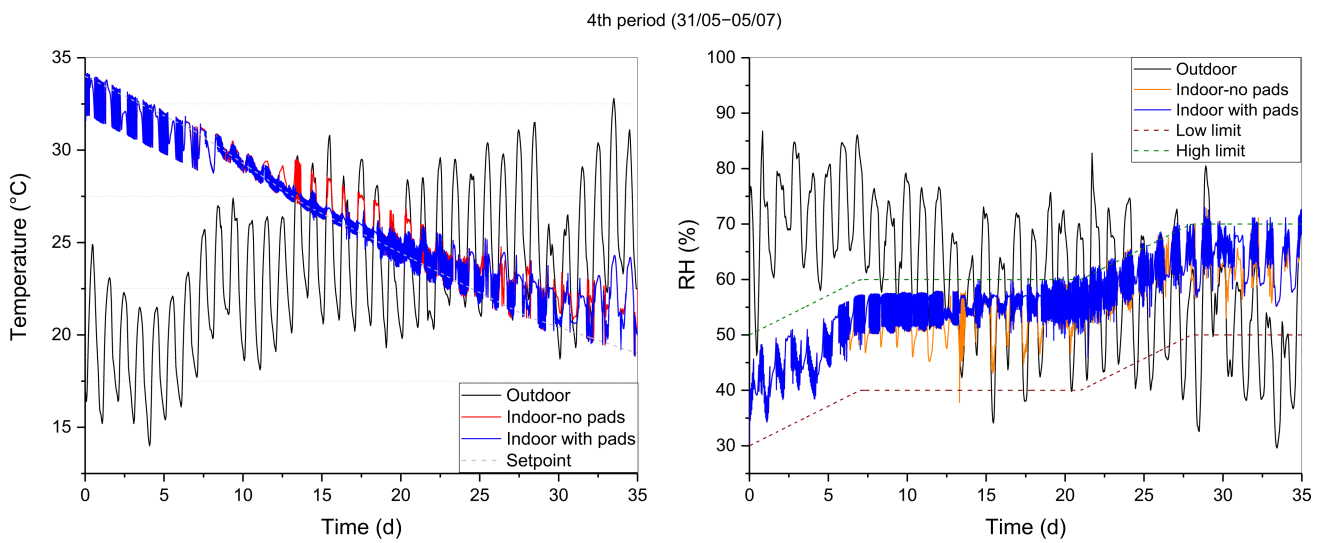


Figure 12. Temperature and relative humidity without and with evaporative pads for the 4th production period (31.05–05.07).

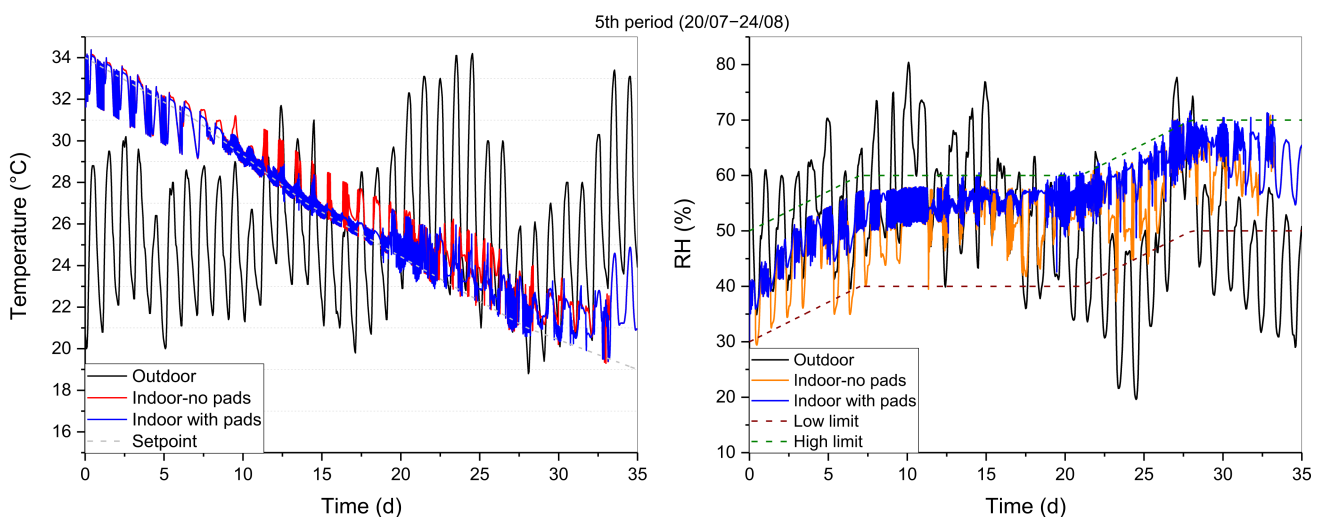


Figure 13. Temperature and relative humidity without and with evaporative pads for the 5th production period (20.07–24.08).

The simulations for these two PPs also provided information about the energy use for each mode (Table 8). As expected, a significant decrease in the energy used for cooling is observed for the two periods, accompanied by a significant increase in energy for dehumidifying. Overall, the total energy use of the HP is slightly reduced for PP4 (−65.3 kWh, or −0.3%) and increased for PP5 (+482.4 kWh, or +2.6%).

The operation of the evaporative cooling system requires the use of a water recirculation pump. The energy use of a such pump is not included in the above results (Table 8). When a pump of 1.1 kW power, and 90% efficiency, is introduced, the total energy use increases by 237.6 kWh during PP4, and 363.0 kWh during PP5. Despite the rise in energy use in this scenario, the potential enhancement of animal welfare could still compensate for the increased costs. Nonetheless, this shortcoming could be mitigated by following a more sophisticated approach in the operation of the free cooling mode, associating the activation of the evaporative cooling with indoor relative humidity.

Table 8. The energy use of each operation mode for the warmest production periods when evaporative pads are also incorporated.

Production Period	Operation Mode	Energy Use [kWh]				
		With ev. Pads	per m ²	without	per m ²	Diff. (%)
4 (31.05–05.07)	Heating	539	0.9	539.7	0.9	−0.1%
	Cooling	6526.3	10.5	9596.7	15.4	−32%
	Dehumidifying	12,085.3	19.4	8859	14.2	36.4%
	Free cooling	150.5	0.2	371.8	0.6	−59.5%
	CO ₂ Ventilation	379.5	0.6	378.5	0.6	0.3%
	TOTAL	19,680.5	31.6	19,745.8	31.7	−0.3%
5 (20.07–24.08)	Heating	190.8	0.3	191.0	0.3	−0.1%
	Cooling	6485.7	19.1	11,884.5	10.4	−45.4%
	Dehumidifying	11,495.6	8.6	5377.9	18.5	113.8%
	Free cooling	290.8	0.9	528.9	0.5	−45%
	CO ₂ Ventilation	379.4	0.6	377.6	0.6	0.5%
	TOTAL	18,842.2	29.5	18,359.8	30.3	2.6%

3.4. Control Aspects

In the present study, a PID-controlled inverter was used to actuate the HP compressor, as opposed to “On/ Off” control strategies which are employed in most applications. Depending on the measured difference between the setpoints and the indoor conditions, the control system adapts the compressor’s speed to match the necessary heating/cooling/dehumidifying loads. This speed variation allows the system to meet the indoor space requirements, achieving higher overall efficiency. The control system could be improved to lead to an even better climate control, as in many cases the fluctuating outdoor conditions lead to short picks or drops of indoor conditions, outside the broilers’ comfort zone. A more meticulous tuning of the PID controller, actuating both HPs and the humidifier, could mitigate this issue. This is identified as a non-trivial task since all different operation scenarios should be taken into consideration, but it could allow even better efficiency and yearly energy use.

In a future work, more advanced control methods, such as model predictive control (MPC), could be also considered. Through this approach, the satisfaction of different sets of constraints could be investigated (e.g., thermal comfort conditions, RES energy use), while the ability to anticipate future events (e.g., weather conditions and energy price fluctuations) could offer additional flexibility to the system.

4. Conclusions

The current study presents a dynamic numerical model in the Simulink environment capable of predicting the thermal needs of a broiler house and simulating the performance of a heat pump (HP) system that adjusts the indoor climate to the desired conditions. The modeled HP is a modular system employing different modules for heating, cooling, and dehumidifying. The climatic conditions as well as the broilers’ heat production are used as model inputs. Furthermore, all the heat exchange mechanisms with the external environment (i.e., convection, conduction, and radiation) were considered. The paper’s main goal was to investigate the energy use of each HP mode under different environmental conditions. To this end, seven different representative production periods (PPs) were simulated based on a typical meteorological year, first by operating the HP alone, and then by also incorporating evaporative cooling pads.

The study estimated overall energy use of 80,506.0 kWh, or 129.4 kWh/m², yearly, with energy needs for dehumidifying (36,515.1 kWh) and cooling (27,010.9 kWh) exceeding those for heating (11,507.8 kWh) by a great amount. The maximum energy used for dehumidifying is 8859.0 kWh during the 4th PP (31.05–05.07), and for cooling 11,884.5 kWh during the 5th PP (20.07–24.08). Maximum heating requirements are 4378.2 kWh during the winter months (PP1). It has been shown that the seasonal coefficient of performance

(SCOP) can reach above 3.1 and 4.8 for heating and dehumidifying, respectively, while the seasonal energy efficiency ratio (SEER) for cooling is above 3.7.

Since the cooling needs proved to contribute significantly to the energy consumption of the broiler house, the HP system was combined with evaporative cooling pads, commonly used in such applications. Simulations were run for the 2 hottest periods of the year, namely, the 4th and 5th PPs. When evaporative pads were introduced in the PPs with the highest cooling requirements, a significant decrease in the energy used for cooling was observed, accompanied by an increase in the necessary energy for dehumidifying. The HP's consumption was reduced during June–July (PP4) and increased during July–August (PP5). The overall energy use was proven to be slightly higher when the operation of the necessary water-recirculating pump was taken into consideration.

The developed model constitutes the first attempt to simulate the dynamic operation of an HP in a broiler house. Its robustness is expected to be enhanced after calibration based on experimental results. The model can be adapted to cover other livestock building cases, serving as a tool for (agricultural) engineers during the pre-study phase of HVAC systems in livestock facilities. Furthermore, it can be useful for both sizing purposes and providing the farmer with energy use and cost data. The simulation results presented in this study reveal the great potential of HP applications in livestock facilities. The precise regulation of the indoor environment of broiler houses with the use of HPs can lead to financial benefits due to lower energy use and enhanced welfare conditions and reveals the need for further investigation into the field of livestock farming.

Author Contributions: Conceptualization, D.M. and P.B.; methodology, P.B. and D.M.; software, D.T., A.G. and P.B.; validation, D.T.; formal analysis, D.T. and A.G.; investigation, D.T., A.G. and P.B.; resources, D.M. and P.P.; data curation, D.T., A.G. and P.B.; writing—original draft preparation, D.T. and A.G.; writing—review and editing, P.P. and D.M.; visualization, A.G.; supervision, D.M.; project administration, D.T.; funding acquisition, D.M. All authors have read and agreed to the published version of the manuscript.

Funding: This research received no external funding.

Conflicts of Interest: The authors declare no conflict of interest.

Appendix A

The coefficients used for calculating the compressor's mass flow rate (kg/h) at different compressor frequencies are given in Table A1 below:

Table A1. Mass flow coefficients at different compressor frequencies.

Compressor Frequency [Hz]	Mass Flow Coefficients				
	c1	c2	c3	c4	c5
25	855.03777430	32.97821384	−0.51148901	0.48433874	−0.04501182
30	1032.75016000	39.83245726	−0.61779769	0.58500446	−0.05436715
35	1211.98482500	46.74541396	−0.72501700	0.68653248	−0.06380261
40	1391.53507800	53.67054270	−0.83242510	0.78823927	−0.07325469
45	1569.74359800	60.54392169	−0.93903056	0.88918603	−0.08263614
50	1744.50242900	67.28424858	−1.04357240	0.98817870	−0.09183598
55	1913.25298500	73.79284047	−1.14452006	1.08376796	−0.10071953
60	2072.97561700	79.95635926	−1.23221931	1.17408353	−0.10974069
65	2220.58147000	85.63806057	−1.33472200	1.25662712	−0.11910551
70	2352.41306900	90.64197225	−1.49523401	1.32859978	−0.12652211
Compressor Frequency [Hz]	Mass Flow Coefficients				
	c6	c7	c8	c9	c10
25	−0.03762171	0.00276231	−0.00136993	−0.00040052	0.00003715
30	−0.04544107	0.00333644	−0.00165466	−0.00048377	0.00004487

Table A1. Cont.

Compressor Frequency [Hz]	Mass Flow Coefficients				
	c6	c7	c8	c9	c10
35	−0.05332740	0.00391548	−0.00194183	−0.00056773	0.00005266
40	−0.06122762	0.00449554	−0.00222950	−0.00065183	0.00006046
45	−0.06906881	0.00507126	−0.00251502	−0.00073531	0.00006820
50	−0.07675821	0.00563585	−0.00279502	−0.00081717	0.00007580
55	−0.08418324	0.00618102	−0.00306539	−0.00089622	0.00008313
60	−0.09165046	0.00671447	−0.00330414	−0.00095883	0.00009514
65	−0.09839886	0.00723777	−0.00347734	−0.00098950	0.00010864
70	−0.10262291	0.00775414	−0.00354423	−0.00099996	0.00010871

The coefficients used for calculating the compressor's power consumption (W) at different compressor frequencies are given in Table A2 below:

Table A2. Power consumption coefficients at different compressor frequencies.

Compressor Frequency [Hz]	Power Consumption Coefficients				
	c1	c2	c3	c4	c5
25	1766.37051400	−103.01710710	185.35068290	−2.72354684	6.01686790
30	2202.26592500	−130.80922570	234.28253400	−3.53204273	7.74371841
35	2640.30392700	−158.73122640	283.44584440	−4.34412559	9.47837012
40	3081.39973600	−186.84146910	332.94336190	−5.16149335	11.22444945
45	3526.46857100	−215.19831360	382.87783420	−5.98584393	12.98558284
50	3976.42564800	−243.86012000	433.35200910	−6.81887527	14.76539674
55	4432.18618500	−272.88524810	484.46863450	−7.66228530	16.56751757
60	4894.47810500	−302.28312230	536.47148270	−8.52074749	18.38457715
65	5372.31938200	−332.37471430	588.65708990	−9.40007229	20.22354832
70	5863.60114500	−363.89016750	640.98191400	−10.30278299	22.12884828

Compressor Frequency [Hz]	Power Consumption Coefficients				
	c6	c7	c8	c9	c10
25	−0.67356199	−0.02101796	0.03304488	−0.01986356	−0.00214472
30	−0.94926763	−0.02750087	0.04375963	−0.02597327	−0.00254993
35	−1.22601772	−0.03401196	0.05451978	−0.03210958	−0.00295749
40	−1.50439147	−0.04056487	0.06534784	−0.03828533	−0.00336824
45	−1.78496806	−0.04717318	0.07626631	−0.04451335	−0.00378304
50	−2.06832670	−0.05385053	0.08729769	−0.05080646	−0.00420273
55	−2.35504658	−0.06061054	0.09846449	−0.05717751	−0.00462817
60	−2.65358853	−0.06715410	0.11009755	−0.06341993	−0.00496922
65	−2.94402933	−0.07292106	0.12276427	−0.06943275	−0.00537774
70	−3.21320416	−0.07793220	0.13658606	−0.07567771	−0.00602051

References

1. Eurostat. Statistics Explained: Agricultural Production—Livestock and Meat. 2022. Available online: <https://ec.europa.eu/eurostat/statistics-explained/index.php?oldid=427096#Poultrymeat> (accessed on 15 March 2023).
2. Augère-Granier, M. *The EU Poultry Meat and Egg Sector: Main Features, Challenges and Prospects: In-Depth Analysis*; European Parliament, Directorate-General for Parliamentary Research Services: Brussels, Belgium, 2019; Available online: <https://data.europa.eu/doi/10.2861/33350> (accessed on 15 March 2023).
3. Da Silva, R.G.; Maia, A.S.C. *Principles of Animal Biometeorology*; Springer: Cham, The Netherlands, 2013; ISBN 978-9400757325.
4. Yahav, S. Regulation of Body Temperature: Strategies and Mechanisms. In *Sturkie's Avian Physiology*, 3rd ed.; Scanes, C.G., Ed.; Academic Press: Cambridge, MA, USA, 2015; pp. 869–905. ISBN 0124071600.
5. Heier, B.T.; Hogåsen, H.R.; Jarp, J. Factors associated with mortality in Norwegian broiler flocks. *Prev. Vet. Med.* **2002**, *53*, 147–158. [[CrossRef](#)]
6. Baarendse, P.J.J.; Kemp, B.; van den Brand, H. Early-age housing temperature affects subsequent broiler chicken performance. *Br. Poult. Sci.* **2006**, *47*, 125–130. [[CrossRef](#)]

7. Blahová, J.; Dobšíková, R.; Straková, E.; Suchý, P. Effect of low environmental temperature on performance and blood system in broiler chickens (*Gallus domesticus*). *Acta Vet. Brno* **2007**, *76*, 17–23. [[CrossRef](#)]
8. Akşit, M.; Altan, Ö.; Karul, A.B.; Balkaya, M.; Özdemir, D. Effects of cold temperature and vitamin E supplementation on oxidative stress, Troponin-T level, and other ascites-related traits in broilers. *Arch. Geflügelkd.* **2008**, *72*, 221–230.
9. Lee, I.-B.; You, B.; Jung, M.; Yun, J.; Chum, J.; Kim, K.; Sung, S. Study on Ventilation Efficiency of a Mechanically Ventilated Broiler House—(II) Winter Season. *J. Livest. Hous. Environ.* **2003**, *9*, 103–112. Available online: <https://www.scopus.com/inward/record.uri?eid=2-s2.0-84876874224&partnerID=40&md5=bd97cb2a25bbee2ba3b4e5690da45a35%0A> (accessed on 15 March 2023).
10. Reece, F.N.; Lott, B.D. The Effects of Temperature and Age on Body Weight and Feed Efficiency of Broiler Chickens. *Poult. Sci.* **1983**, *62*, 1906–1908. [[CrossRef](#)] [[PubMed](#)]
11. De Oliveira, R.F.M.; Donzele, J.L.; De Abreu, M.L.T.; Ferreira, R.A.; Vaz, R.G.M.V.; Cella, P.S. Effects of temperature and relative humidity on performance and yield of noble cuts of broilers from 1 to 49 days old. *Rev. Bras. Zootec.* **2006**, *35*, 797–803. [[CrossRef](#)]
12. Okelo, P.O.; Carr, L.E.; Harrison, P.C.; Douglass, L.W.; Byrd, V.E.; Wabeck, C.W.; Schreuders, P.D.; Wheaton, F.W.; Zimmermann, N.G. Effectiveness of a novel method to reduce heat stress in broilers: A cool roost system. *Trans. ASAE* **2003**, *46*, 1675–1683. [[CrossRef](#)]
13. Han, H.; Kim, K.; Jang, K.J.; Han, G.S.; Lee, I.B. Energy consumption and indoor environment of broiler houses with energy recovery ventilators. *Appl. Eng. Agric.* **2013**, *29*, 751–759. [[CrossRef](#)]
14. Bokkers, E.A.M.; van Zanten, H.H.E.; van den Brand, H. Field study on effects of a heat exchanger on broiler performance, energy use, and calculated carbon dioxide emission at commercial broiler farms, and the experiences of farmers using a heat exchanger. *Poult. Sci.* **2010**, *89*, 2743–2750. [[CrossRef](#)]
15. Paris, B.; Vandorou, F.; Tyriss, D.; Balafoutis, A.T.; Vaiopoulos, K.; Kyriakarakos, G.; Manolakos, D.; Papadakis, G. Energy Use in the EU Livestock Sector: A Review Recommending Energy Efficiency Measures and Renewable Energy Sources Adoption. *Appl. Sci.* **2022**, *12*, 2142. [[CrossRef](#)]
16. de Vries, M.; de Boer, I.J.M. Comparing environmental impacts for livestock products: A review of life cycle assessments. *Livest. Sci.* **2010**, *128*, 1–11. [[CrossRef](#)]
17. Costantino, A.; Fabrizio, E.; Biglia, A.; Cornale, P.; Battaglini, L. Energy Use for Climate Control of Animal Houses: The State of the Art in Europe. *Energy Procedia* **2016**, *101*, 184–191. [[CrossRef](#)]
18. Costantino, A.; Fabrizio, E.; Ghiggini, A.; Bariani, M. Climate control in broiler houses: A thermal model for the calculation of the energy use and indoor environmental conditions. *Energy Build.* **2018**, *169*, 110–126. [[CrossRef](#)]
19. Baxevanou, C.; Fidaros, D.; Bartzanas, T.; Kittas, C. Energy Consumption and Energy Saving Measures in Poultry. *Energy Environ. Eng.* **2017**, *5*, 29–36. [[CrossRef](#)]
20. Daskalov, P.I.; Arvanitis, K.G.; Pasgianos, G.D.; Sigrimis, N.A. Non-linear Adaptive Temperature and Humidity Control in Animal Buildings. *Biosyst. Eng.* **2006**, *93*, 1–24. [[CrossRef](#)]
21. Alimuddin, I.; Seminar, K.B.; Subrata, I.D.M.; Sumiati, I.; Nomura, N. A Supervisory Control System for Temperature and Humidity in a Closed House Model for Broilers. *Int. J. Electr. Comput. Sci. IJECs-IJENS* **2011**, *11*, 33–41. Available online: <https://citeseerx.ist.psu.edu/document?repid=rep1&type=pdf&doi=42c624cb31dd077a66b7310b7f1c9bd8a3853ed3> (accessed on 15 March 2023).
22. Daskalov, P.I. Prediction of Temperature and Humidity in a Naturally Ventilated Pig Building. *J. Agric. Eng. Res.* **1997**, *68*, 329–339. [[CrossRef](#)]
23. Lahlouh, I.; Elakkary, A.; Nacer, S. PID Controller of a MIMO System Using Ant Colony Algorithm and Its Application to a Poultry House System. In Proceedings of the 2019 5th International Conference on Optimization and Applications (ICOA), Kenitra, Morocco, 25–26 April 2019; pp. 1–7. [[CrossRef](#)]
24. Lahlouh, I.; Rerhrhaye, F.; Elakkary, A.; Sefiani, N. Experimental implementation of a new multi input multi output fuzzy-PID controller in a poultry house system. *Heliyon* **2021**, *7*, 8440. [[CrossRef](#)]
25. European Commission. *Directive 2012/27/EU on Energy Efficiency*; European Commission: Brussels, Belgium, 2012. Available online: <http://data.europa.eu/eli/dir/2012/27/oj> (accessed on 15 March 2023).
26. European Commission. *Directive 2010/31/EU on the Energy Performance of Buildings*; European Commission: Brussels, Belgium, 2010; Available online: <http://data.europa.eu/eli/dir/2010/31/oj> (accessed on 15 March 2023).
27. Tyriss, D.; Gkountas, A.; Bakalis, P.; Panagakis, P.; Manolakos, D. A dynamic heat pump model for precise environment control of a broiler house in Northern Greece. In Proceedings of the AgEng-LAND.TECHNIK 2022, Berlin, Germany, 22–23 November 2022; pp. 485–491, ISBN 0083-5560.
28. MathWorks. Simulation and Model-Based Design. 2022. Available online: <https://www.mathworks.com/products/simulink.html> (accessed on 15 March 2023).
29. Mathworks. Simscape™ Reference R2022b. 2022. Available online: https://www.mathworks.com/help/pdf_doc/simscape/index.html (accessed on 15 March 2023).
30. Kalogirou, S.A. *Solar Energy Engineering*, 2nd ed.; Elsevier: Amsterdam, The Netherlands, 2014; ISBN 9780123972705.
31. Tsilingiridis, G.; Papakostas, K. Investigating the relationship between air and ground temperature variations in shallow depths in northern Greece. *Energy* **2014**, *73*, 1007–1016. [[CrossRef](#)]
32. Nicolaides & Kountouris Metal Company Ltd. Polyurethane Insulating Panels. Available online: https://www.nkmetal.com.cy/images/pages/products_polyurethane_panels/Polyurethane%20leaflet%20ENG.pdf (accessed on 15 March 2023).

33. Manolakos, D.; Panagakis, P.; Bartzanas, T.; Bouzianas, K. Use of heat pumps in HVAC systems for precise environment control in broiler houses: System's modeling and calculation of the basic design parameters. *Comput. Electron. Agric.* **2019**, *163*, 104876. [CrossRef]
34. Reilly, A.; Kinnane, O. The impact of thermal mass on building energy consumption. *Appl. Energy* **2017**, *198*, 108–121. [CrossRef]
35. Cobb-Vantress. *COBB Broiler Management Guide*; Cobb: Siloam Springs, AK, USA, 2021.
36. Lohmann Meat. *Broiler Stock Performance Objectives*; Aviagen: Huntsville, AL, USA, 2007.
37. Sallvik, K.; Pedersen, S. Animal and heat production. In *CIGR Handbook of Agricultural Engineering, Volume II: Animal Production & Aquacultural Engineering*; Bartali, E.H., Ed.; American Society of Agricultural Engineers: St. Joseph, MI, USA, 1999; Volume 2, pp. 31–88. ISBN 0929355989.
38. Rojano, F.; Bournet, P.E.; Hassouna, M.; Robin, P.; Kacira, M.; Choi, C.Y. Modelling heat and mass transfer of a broiler house using computational fluid dynamics. *Biosyst. Eng.* **2015**, *136*, 25–38. [CrossRef]
39. Carrier Air Conditioning Company. *Carrier Handbook of Air Conditioning System Design*; McGraw-Hill Book Company: New York, NY, USA, 1966; ISBN 007010090X.
40. Mathworks. Moist Air Models. Simscape™ Reference R2022b. Available online: <https://www.mathworks.com/help/simscape/moist-air-models.html> (accessed on 15 March 2023).
41. Mathworks. Two-Phase Fluid Models. Simscape™ Reference R2022b. Available online: <https://www.mathworks.com/help/simscape/two-phase-fluid-models.html> (accessed on 15 March 2023).
42. Mathworks. Thermal Liquid Models. Simscape™ Reference R2022b. Available online: <https://www.mathworks.com/help/simscape/thermal-liquid-models.html> (accessed on 15 March 2023).
43. BITZER GmbH. Semi-Hermetic Reciprocating Compressor 6GE-34. Available online: <https://www.bitzer.de/gr/en/> (accessed on 15 March 2023).
44. BITZER GmbH. Bitzer Software. Available online: <https://www.bitzer.de/websoftware/> (accessed on 15 March 2023).

Disclaimer/Publisher's Note: The statements, opinions and data contained in all publications are solely those of the individual author(s) and contributor(s) and not of MDPI and/or the editor(s). MDPI and/or the editor(s) disclaim responsibility for any injury to people or property resulting from any ideas, methods, instructions or products referred to in the content.